trigonal face of $Cr(sen)^{3+}$ in its ground-state geometry and in the trigonal-prismatic geometry. The results shown in Figure 7 indicate that such an association is about 17 kJ mol^{-1} less repulsive in the trigonally distorted complex than in the ground state. This suggests that trigonal distortion, at least of $Cr(sen)^{3+}$, could facilitate ligand substitution as well as excited-state relaxation. To the degree that doubly occupied microstates contribute to a (^{2}E)Cr(III) electronic structure in a D_{3h} microenvironment, there could also be a stronger bond between (^{2}E)Cr(III) and the entering group in the D_{3h} than in the O_h geometry, so that association with solvent and the trigonal distortion might interact synergistically to promote the large amplitude trigonal distortions that result in excited-state relaxation. The present information does not allow resolution of such details. Our observations do indicate that the trigonal twist itself (without solvent association) is probably sufficient to induce excited state relaxation and that association with the solvent, if it occurs, may well occur after the electronically excited system is far into the relaxation channel.[42]

(42) Note that the several reports of photoracemization of Cr(III) complexes that have D_3 symmetry[33] could be evidence for very large amplitude of trigonal distortions in (^{2}E)Cr(III) relaxation: (a) Kane-Maguire, N. A. P.; Langford, C. H. *J. Am. Chem. Soc.* **1972**, *94*, 2125. (b) Kane-Maguire, N. A. P.; Langford, C. H. *Inorg. Chem.* **1976**, *15*, 464. (c) Kane-Maguire, N. A. P.; Phifer, J. E.; Toney, C. G. *Inorg. Chem.* **1976**, *15*, 593.

Conclusions. We have shown that introduction of trigonal strain into $Cr(en)_3^{3+}$ by encapsulating one trigonal face with a neopentyl moiety results in many orders of magnitude decrease in the ambient solution ^{2}E excited-state lifetime of the resulting $Cr(sen)^{3+}$ complex. The chromium microenvironments differ very little in the $Cr(en)_3^{3+}$ and $Cr(sen)^{3+}$ complexes, and this structural similarity is reflected in the very similar electronic properties of the two complexes. The one notable difference between them is the tendency of the coordinated sen ligand to twist along a trigonal axis. Thus, these two complexes fit nicely into a pattern of behavior that has begun to emerge for (hexaam(m)ine)chromium(III) complexes: large-amplitude trigonal distortions facilitate thermally activated (^{2}E)Cr(III) excited-state relaxation.

Acknowledgment. We wish to thank the AT&T company for their gift of the 3b2 computers, terminals, and operating software. The X-ray diffractometer was purchased through an NSF equipment grant to Wayne State University.

Registry No. $[Cr(sen)]Br_3$, 134567-53-6; $[Rh(sen)]Cl_3$, 134567-54-7; $[Rh(sen)]Br_3$, 134567-55-8; $Cr([9]aneN_3)_2^{3+}$, 93714-28-4; $Cr([9]aneN_3CH_2^-)_2^{3+}$, 95388-39-9; $Cr(TAP[9]aneN_3)^{3+}$, 125454-25-3; $Cr(TAE[9]aneN_3)^{3+}$, 125454-24-2; $Cr(en)_3^{3+}$, 15276-13-8; $Cr(NH_3)_6^{3+}$, 14695-96-6; $Cr([9]aneN_3)(NH_3)_3^{3+}$, 116745-22-3.

Supplementary Material Available: For $[Cr(sen)]Br_3$, Tables B and C, listing thermal parameters and hydrogen atomic parameters (2 pages); Table A, listing observed and calculated structure factors (23 pages). Ordering information is given on any current masthead page.

Contribution from the Departments of Chemistry, Grinnell College, Grinnell, Iowa 50112, and University of Vermont, Burlington, Vermont 05405

NMR and Crystallographic Determination of Stereoselectivity in the Coordination of Prochiral Olefinic Alcohols in Mixed Olefin–Amino Acid Complexes of Platinum(II)

Luther E. Erickson,*,† Garth S. Jones,† Jason L. Blanchard,† and Kazi J. Ahmed‡

Received August 17, 1990

NMR spectroscopy (^{1}H, ^{13}C, and ^{195}Pt) was employed to determine the effect of metal-centered stereochemistry on the stereoselectivity of coordination of prochiral olefinic alcohols by comparing the equilibrium distribution of diastereomers of cis- and trans(N,olefin) isomers for mixed olefin–amino acid complexes of general formula Pt(amino acid)(olefin)Cl for amino acid = glycine, α-aminoisobutyric acid, sarcosine (sar), and (*S*)-proline (*S*-pro) and olefin = allyl alcohol, 3-buten-2-ol, and 2-methyl-3-buten-2-ol (2-mb). In agreement with earlier reports, the stereoselectivity of olefin coordination is not significant (ratio of diastereomers 1.0–1.3) for any of the trans(N,olefin) species. However, for cis(N,olefin) isomers of N-chiral sarcosine and (*S*)-proline, the stereoselectivity is substantial, especially for 2-mb for which the preferred diastereomers predominate by >40/1. X-ray structures of the preferred isomers of *cis(N-olefin)*-Pt(sar)(2-mb)Cl (space group *Pcab* with a = 10.705 (3) Å, b = 13.671 (3) Å, c = 15.908 (3) Å, Z = 8, and R = 0.046), of *trans(N,olefin)*-Pt(*S*-pro)(2-mb)Cl (space group $P2_12_12_1$ with a = 6.955 (4) Å, b = 9.971 (4) Å, c = 19.060 (9) Å, Z = 4, and R = 0.069), and of the related dimethyl sulfoxide complex *cis(N,S)*-Pt(sar)(Me_2SO)Cl (space group *Pbca* with a = 10.290 (3) Å, b = 12.398 (3) Å, c = 16.231 (6) Å, Z = 8, and R = 0.041) were determined in order to establish the stereochemistry of the preferred isomers (olefin-*R*, amino acid N-*S* in both cases) and to identify intramolecular interactions, including hydrogen bonding, that contribute to the large stereoselectivities observed for cis(N,olefin) species.

Introduction

The asymmetric template available in a metal atom and its attached ligands provides a simple and convenient method for achieving stereoselectivity in the coordination of another chiral or prochiral ligand. Such stereoselectivity of coordination can be exploited in the development of methods for asymmetric synthesis[1] and for separation of isomers,[2] including optical isomers.[3] Though steric factors are no doubt responsible for observed differences in selectivity of binding, the degree of stereoselectivity for the binding of a particular ligand with a given chiral template is difficult to predict with any certainty. This project, part of a systematic study of the interaction between metal-centered and ligand-centered stereochemistry, was undertaken to provide such fundamental data for mixed amino acid–olefin–platinum(II) complexes of general formula Pt(amino acid)(olefin)Cl, which can exist in two stable geometric isomers denoted trans(N,olefin) (**1**) and cis(N,olefin) (**2**).

Saito and co-workers have reported investigations of both stereochemistry and of olefin exchange in several mixed olefin–amino acid complexes by NMR and optical spectroscopy, including

† Grinnell College.
‡ University of Vermont.

(1) Morrison, J. D., Ed. *Asymmetric Synthesis*; Academic Press: New York, 1985; Vol. 5.
(2) Jacques, J.; Collet, R.; Wilen, S. H. *Enantiomers, Racemates, and Resolutions*; Wiley-Interscience: New York, 1981.
(3) As employed by Cope et al. for the resolution of cyclooctadiene and other chiral olefins: Cope, A. C.; Gaellin, C. N.; Johnson, W. H. *J. Am. Chem. Soc.* **1962**, *84*, 3191. Cope, A. C.; Careso, E. A. *J. Am. Chem. Soc.* **1966**, *88*, 1711.

0020-1669/91/1330-3147$02.50/0

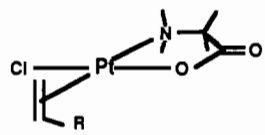

1

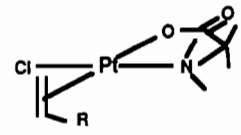

2

ORD and CD spectral measurements.[4] In general, the degree of selectivity of coordination of the prochiral olefins at equilibrium that they reported was not great, although specific diastereomers were sometimes obtained by selective precipitation[5] and stereoselective coordination of prochiral olefins may be favored kinetically.[6] However, most of their studies employed trans(N,olefin) isomers of general formula Pt(amino acid)(olefin)Cl, for which the chiral centers of the olefin and the amino acid portions are spatially well separated. The only system in which cis(N,olefin) and trans(N,olefin) isomers have been directly compared is the (*S*)-alanine/styrene system,[7] for which the degree of stereoselectivity is modest for both cis ((*R*)-styrene/(*S*)-styrene = 1.27) and trans ((*S*)-styrene/(*R*)-styrene = 1.14) isomers. Moreover, for these alanine complexes, the chiral center at the α-C of the amino acid is also relatively remote from the chiral center of the coordinated olefin for both cis and trans isomers, so the low degree of stereoselectivity is again not surprising.

Both cis and trans isomers of several mixed amino acid–olefin complexes of the water-soluble alcoholic olefins allyl alcohol (allOH) (**3**), 3-buten-2-ol (3-but) (**4**), and 2-methyl-3-buten-2-ol (2-mb) (**5**)[8] have been included in this investigation of the ste-

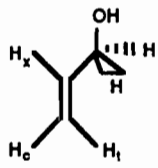

3

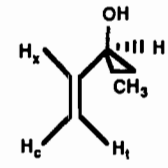

4

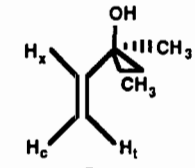

5

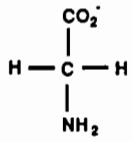

6

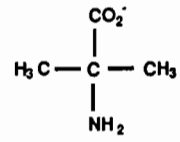

7

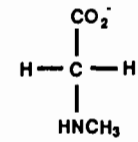

8

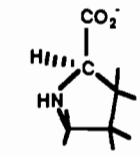

9

reoselectivity of olefin coordination. Both achiral amino acids, glycine (gly) (**6**) and α-aminoisobutyric acid (aba) (**7**), and N-chiral amino acids, sarcosine (sar) (**8**) and (*S*)-proline (*S*-pro) (**9**), have been included in the study in order to establish reliable NMR criteria for assignment of stereochemistry and to compare intraligand and interligand interactions for coordinated 3-but, which contains two chiral carbons. NMR spectra (^{1}H, ^{13}C, and ^{195}Pt) have been employed to determine the equilibrium composition of diastereomeric species that are possible for 16 of the 24 combinations of cis and trans geometries for three olefins with four amino acids.

X-ray crystal structures of two of the complexes, *trans*(*N*,2-*mb*)-Pt(*S*-pro)(2-mb)Cl and *cis*(*N*,2-*mb*)-Pt(sar)(2-mb)Cl, have been determined in order to establish the stereochemistry of the single isomer of each that was isolated under specific experimental conditions and, thereby, to identify significant factors that influence the equilibrium stereoselectivities observed. These structures, along with that of the closely parallel dimethyl sulfoxide–amino acid complex *cis*(*N*,*S*)-Pt(sar)(Me_2SO)Cl are included in this report. Rates of olefin exchange have also been determined for several of the complexes, in part to ensure that equilibration of isomers has been achieved under the conditions employed in the study. Details of that kinetic study will be reported separately.[9] Rates of internal rotation about the Pt–olefin bond and the equilibrium rotamer distributions of coordinated olefins in some of these compounds are also being investigated at this time.

Scheme I

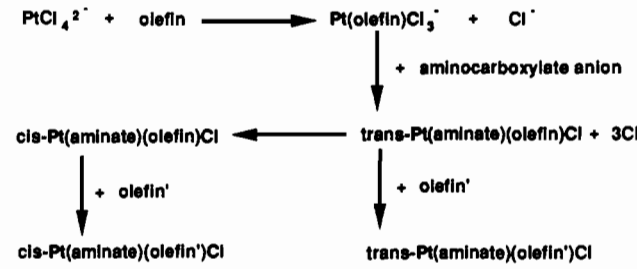

Table I. Elemental Analysis (%) for Pt(aminate)(olefin)Cl Compounds

compd (formula)	calculated			observed		
	C	H	N	C	H	N
trans-Pt(aba)(2-mb)Cl ($PtC_9H_{18}NO_3Cl$)	25.81	4.33	3.34	25.90	4.38	3.31
trans-Pt(aba)(CH_2=CH_2)Cl ($PtC_6H_{12}NO_2Cl$)	19.88	3.35	3.88	20.05	3.37	3.87
cis-Pt(aba)(allOH)Cl ($PtC_7H_{14}NO_3Cl$)	21.51	3.61	3.58	21.60	3.63	3.53
cis-Pt(sar)(2-mb)Cl ($PtC_8H_{16}NO_3Cl$)	23.73	3.98	3.46	23.82	3.98	3.45
trans-Pt(*S*-pro)(2-mb)Cl ($PtC_{10}H_{20}NO_3Cl$)	27.74	4.65	3.23	27.90	4.24	3.24

Experimental Details

Materials. The olefins and amino acids employed in the synthesis of the compounds, reported here are all commercially available compounds (Aldrich Chemical Co.). The source of the platinum was K_2PtCl_4, obtained from Englehard Industries, Ltd. Deuterated solvents and other standard supplies for NMR spectroscopy were similarly obtained from Aldrich Chemical Co.

Synthesis of Complexes. The general approach to synthesis of these compounds is outlined in Scheme I.[10] Stock solutions of the 1:1 complexes Pt(olefin)Cl_3^- of allyl alcohol and 2-mb were prepared by adding a slight excess of free olefin (1.05 mmol/mmol of Pt) to a 0.25 M solution of K_2PtCl_4 in 0.01 M aqueous HCl. This solution was equilibrated at room temperature or at about 50 °C until the bright yellow color of the Zeise's salt analogue indicated essentially complete reaction (from 2–3 h for allyl alcohol at 50 °C to 1 week for 2-mb at room temperature).[11] A portion of this solution was then added to the potassium salt of one of the amino acids (1 mol of amino acid/mol of Pt) that had been neutralized with the calculated volume of standardized KOH (~1 M). After a few minutes at room temperature to permit rapid displacement of the chloride trans to the olefin,[12] the solution was chilled in an ice bath or refrigerator to precipitate the *trans*-Pt(aminate)(olefin)Cl isomer. The solid trans isomer was separated promptly by suction filtration to prevent isomerization to the cis isomer, washed with a minimum of cold 0.001 M HCl, and dried in a desiccator. If the trans isomer failed to precipitate promptly, or after the yield of trans isomer had been filtered off, the reaction mixture was heated to 40–50 °C to convert any remaining trans to the corresponding thermodynamically favored cis isomer, a conversion typically marked by a fading of the yellow color of the trans isomer as

(4) Highlights of earlier work in this area are reviewed in the following: Saito, K.; Kashiwabara, K. *J. Organomet. Chem.* **1987**, *330*, 291. Saito, K. In *Stereochemistry of Optically Active Transition Metal Compounds*; Douglas, B. E., Saito, Y., Ed.; American Chemical Society: Washington, DC, 1980; Chapter 5.
(5) Kanya, K.; Fujita, J.; Nakamoto, K. *Inorg. Chem.* **1971**, *10*, 1699.
(6) Terai, Y.; Kido, H.; Kashiwabara, K.; Saito, K. *Bull. Chem. Soc. Jpn.* **1978**, *512*, 3245.
(7) Shirado, S.; Sudo, Y.; Yamoguchi, Y.; Iwayomagi, T.; Saito, Y. *Organomet. Chem.* **1976**, *121*, 93.
(8) Comparative NMR properties of *cis*- and *trans*-Pt(PR_3)(olefin)Cl_2 isomers of these three olefins are reported by: Briggs, J. R.; Croker, C.; McDonald, W. S.; Shaw, B. L. *J. Chem. Soc., Dalton Trans.* **1980**, 64.
(9) Erickson, L. E.; Bemis, J.; Elout, M. Manuscript in preparation.
(10) Erickson, L. E.; Brower, D. C. *Inorg. Chem.* **1982**, *21*, 838.
(11) Favorable equilibrium constants ensure essentially complete conversion of K_2PtCl_4 to the corresponding Zeise's anion analogue in the presence of free olefin: Hartley, F. R.; Venanzi, L. M. *J. Chem. Soc. A* **1967**, 330.
(12) Cavoli, P.; Graziani, R.; Casellato, V.; Uguagliate, P. *Inorg. Chim. Acta* **1986**, *111*, L35.

Table II. Summary of Crystallographic Data for Pt(*S*-pro)(2-mb)Cl (**10**), Pt(sar)(2-mb)Cl (**11**), and Pt(sar)(DMSO)Cl (**12**)

	10	**11**	**12**
chem formula	$C_{10}H_{17}NO_3ClPt$	$C_8H_{16}NO_3ClPt$	$C_5H_{12}NO_3SClPt$
fw	429.81	404.78	396.78
a, Å	6.955 (4)	10.705 (3)	10.290 (3)
b, Å	9.971 (4)	13.671 (3)	12.398 (3)
c, Å	19.060 (9)	15.908 (3)	16.231 (6)
Z	4	8	8
V, Å^3	1321 (1)	2328 (1)	2070 (1)
space group	$P2_12_12_1$ (No. 19)	*Pcab* (No. 61)	*Pbca* (No. 61)
T, °C	23	23	23
λ, Å	0.71069	0.71069	0.71069
ρ_{calcd}, g cm^{-3}	2.16	2.31	2.55
μ, cm^{-1}	109.3	123.9	141.2
R^a	0.069	0.046	0.041
$R_w{}^b$	0.069	0.047	0.045

$^a R = \sum||F_o| - |F_c||/\sum|F_o|$. $^b R_w = [\sum w(|F_o| - |F_c|)^2/\sum w|F_o|^2]^{1/2}$; $w = 1/\sigma^2(|F_o|) + 0.002(|F_o|^2)$.

it is converted to the colorless or paler yellow cis isomer. Progess of the isomerization reactions was followed by monitoring NMR spectral changes (^{1}H, ^{13}C, or ^{195}Pt). Some decomposition yielding black deposits of platinum sometimes occurred, especially at elevated temperatures for 2-mb complexes.

Either allyl alcohol or 2-mb complexes of both cis and trans isomers of each of the four amino acids gly, aba, and sar were prepared by this procedure. Single isomers of *cis*-Pt(sar)(2-mb)Cl and *trans*-Pt(*S*-pro)(2-mb)Cl were obtained in the synthesis, while a mixture of diastereomers of *trans*-Pt(sar)(2-mb)Cl separated as an oil. Isomerically pure *cis*-Pt(*S*-pro)(2-mb)Cl was obtained from the allyl alcohol analogue by allowing a reaction mixture containing (*S*)-proline and allyl alcohol to equilibrate for 3 days at room temperature after addition of the (*S*)-proline to yield a mixture of trans and cis isomers of Pt(*S*-pro)(allOH)Cl (as revealed by ^{13}C and ^{195}Pt NMR spectra). After rotary evaporation of solvent, the mixed solids were treated repeatedly with a 10-fold excess of 2-mb in methanol, followed each time by evaporation of solvent and excess olefin. Subsequent treatment of the solid with methanol removed the more soluble *trans* isomers to yield the white solid *cis*-Pt(*S*-pro)(2-mb)Cl. Elemental analyses of some of the previously unreported complexes are reported in Table I.

Solutions of all of the 3-but isomers and of some of the other complexes for NMR spectral analysis were prepared from the isolated allOH or 2-mb complexes having the corresponding geometry and amino acid by simple exchange in methanol (Scheme I). Typically, 5–10 mg (0.01–0.02 mmol) of solid was dissolved in a minimum of methanol and a large excess (100 mg ≅ 1 mmol) of 3-but was added. After a few minutes were allowed to ensure olefin equilibration, the solution was rotary evaporated to dryness at 25–40 °C and the treatment was repeated to ensure essentially complete replacement of the original olefin. Two additional treatments with methanol, each followed by evaporation to dryness in vacuo, assured removal of excess olefins and solvent, and the resulting solid was dissolved in 0.50–1.0 mL of methanol-d_4 for spectral measurements. For samples prepared from pure isomers, equilibration of diastereomers was ensured by adding a small quantity of free olefin and reexamination of the proton spectrum after several hours at room temperature.

NMR Spectra. Proton, ^{13}C, and ^{195}Pt NMR spectra of 0.01–0.03 M solutions of the compounds in methanol-d_4 were obtained with a Bruker AF300 NMR spectrometer, equipped with a superconducting magnet and operating at 300 MHz for proton spectra. Several thousand scans were typically recorded for the ^{13}C spectra in order to improve chances of locating the ^{195}Pt satellites resulting from coupling between ^{13}C and ^{195}Pt nuclei ($I = {}^1/_2$, 33.4% abundance). In some cases these details were only evident in the spectra of solutions more concentrated than the usual 0.01–0.03 M. Similarly, 10000–100,000 scans at 100000 Hz (1562 ppm) sweep width were usually employed to obtain good quality Pt-195 spectra of samples contained in either 5- or 10-mm sample tubes. Most spectra were recorded at 295 ± 2 K, without temperature control of the samples.

Spectra were processed by software resident in the Aspect-3000 computer of the spectrometer or were transferred to an AST-Premium PC for storage and processing by PC-NMR.[13] Chemical shifts of ^{1}H and ^{13}C were based on internal standards (^{1}H, center of CHD_2 of solvent methanol-d_4 = 3.300 ppm; ^{13}C, center of methanol-d_4 heptet = 49.00 ppm), while those of ^{195}Pt were based on external standards (singlet from Na_2PtCl_6 = 0 or from K_2PtCl_4 = −1620 ppm.)[14]

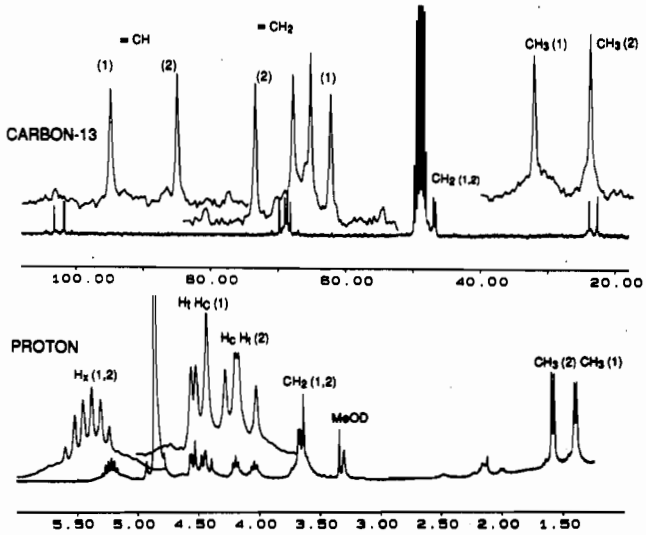

Figure 1. Proton (300 MHz) and carbon-13 (75 MHz) NMR spectra of equilibrium mixtures of isomers of Pt(gly)(3-but)Cl in methanol-d_4, showing assignments of peaks to the two diastereomers.

Solid-State Structures. A summary of crystallographic data for the three structures reported here is given in Table II. Additional details of the structure analysis are given below.

Crystal Growth. Pale yellow crystals of *trans*-Pt(*S*-pro)(2-mb)Cl (**10**), the initial product of the reaction of a 1:1 mixture of K[Pt(2-mb)Cl$_3$] and (*S*)-prolinate in water, were obtained by cooling a solution of **10** in methanol to −30 °C. Most of the crystals were twinned or cracked. After several attempts, an irregularly shaped crystal suitable for analysis was obtained by cleaving a larger crystal. Colorless cube-shaped crystals of *cis*-Pt(sar)(2-mb)Cl (**11**) were grown by layering heptane over an equal volume of a saturated solution of the compound in ethanol (about 0.01 M). The mixture was cooled undisturbed at −30 °C for 3 days. A crystal of approximate dimension 0.35 × 0.30 × 0.30 mm was chosen for X-ray analysis. Slow evaporation of a saturated solution of *cis*(*N*,*S*)-Pt(sar)(Me$_2$SO)Cl (**12**) in 0.01 M HCl over 3 days produced a large number of colorless, parallelepiped-shaped crystals. A crystal of approximate dimension 0.30 × 0.20 × 0.40 mm was chosen for X-ray analysis.

Data Collection and Refinement. The crystals were mounted on glass fibers with epoxy resin. Cell constants and the orientation matrix for intensity data collection of each crystal were based on the setting angles of 17 centered reflections. Acceptable ω scans of several strong low angle reflections were obtained for each crystal. ω–2θ type scans over various 2θ ranges (given in Table II) were used for data collection. The structures were solved by a combination of direct methods and standard heavy-atom Fourier techniques (Nicolet SHELXTL PLUS crystallographic package). Full-matrix least-squares refinement was carried out with anisotropic thermal parameters for all non-hydrogen atoms. Hydrogen atoms were placed in calculated positions (d_{C-H} = 0.95 Å).

Systematic absences in the reflection data of *trans*-Pt(*S*-pro)(2-mb)Cl (**10**) indicated the orthorhombic space group $P2_12_12_1$ (No. 19), with Z = 4. C(4) (Figure 4) showed positional disorder, and the disorder was modeled by accommodating the two equivalent puckering positions of the N(1)–C(1)–C(3)–C(4)–C(4′)–C(5) ring. Each of the C(4) and C(4′) atoms was given 50% occupancy. Figure 4 shows only one form of the pucker. The final difference Fourier map showed four peaks of intensity 3.5–3 e/Å^3 near the Pt atom (0.6–0.8 Å). Refinement converged at R = 0.069 and R_w = 0.069. No absorption correction was applied.

On the basis of the systematic absences in the reflection data, the orthorhombic space groups *Pcab* (a nonstandard setting of *Pbca*, No. 61) and Pbca (No. 61) were chosen for *cis*-Pt(sar)(2-mb)Cl (**11**) and *cis*-(*N*,*S*)-Pt(sar)(Me$_2$SO)Cl (**12**), respectively. The final difference Fourier maps showed two peaks of intensity 2 e/Å^3 near the Pt atoms (~0.9 Å for **11** and 1.3 Å for **12**). Refinement converged at R = 0.046 and R_w = 0.047 for **11** and R = 0.041 and R_w = 0.045 for **12**. No absorption correction was applied.

(13) PC-NMR, a copyrighted NMR data-processing software package is available from T. Farrar, Chemistry Department, University of Wisconsin, Madison, WI.

(14) Brevard, C.; Granger, P. *Handbook of High Resolution Multinuclear NMR*; Wiley-Interscience: New York, 1981; p 200.

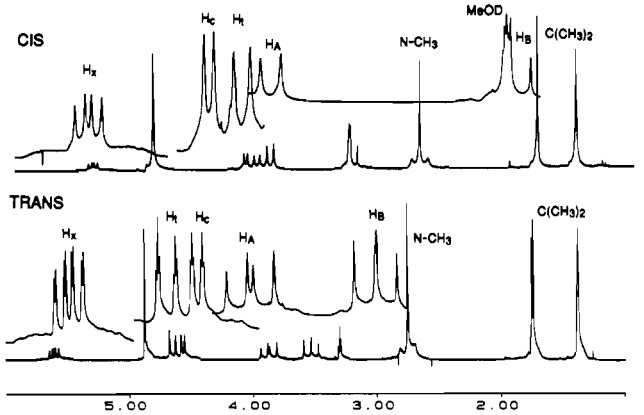

Figure 2. Comparative 300-MHz proton NMR spectra of methanol-d_4 (pentet at 3.30 ppm for CHD_2) solutions of cis(N,olefin) and trans(N,olefin) isomers of Pt(sar)(2-mb)Cl. Note the details of the expansions (especially H_A and H_B of glycinate ring protons), which show two species for the trans isomer but only one species for the cis isomer.

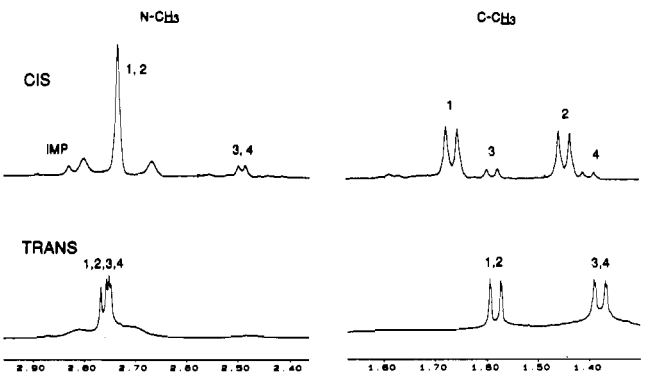

Figure 3. Comparative 300-MHz proton NMR spectra of the methyl region (C–CH_3 doublets and N–CH_3 singlets with broad ^{195}Pt satellites) of methanol-d_4 solutions of cis(N,olefin) and trans(N,olefin) isomers of Pt(sar)(3-but)Cl, showing the presence and relative concentrations of the four diastereomers (labeled 1–4) of each isomer.

Results

Systematic Trends in Chemical Shifts and Coupling Constants. Systematic differences in ^{1}H, ^{13}C, and ^{195}Pt NMR parameters have enabled us to identify and quantify equilibrium isomer distributions for both cis and trans species for all of the combinations examined. Figures 1–3 illustrate important spectral distinctions that were employed in the analysis. Figure 1 illustrates the effect of a second chiral center in the olefin 3-but on the ^{1}H and ^{13}C NMR spectra of *trans*-Pt(gly)(3-but)Cl. Comparable relative concentrations of both *R,S* and *S,S* (or of NMR-indistinguishable *S,R* and *R,R*) diastereomers are evident in *both* ^{1}H and ^{13}C spectra. Figure 2 illustrates the sharply contrasting behavior of *cis*- and *trans*-Pt(sar)(2-mb)Cl, with one chiral center in each ligand. Two diastereomers are possible for each metal-centered isomer, and both isomers are evident in the spectrum of the equilibrated sample of the trans isomer. However, only a single isomer is evident in the ^{1}H NMR spectrum of *cis*-Pt(sar)(2-mb)Cl (and in the ^{13}C spectrum of the same solution). Figure 3 compares the distribution of the four diastereomers of *cis*- and *trans*-Pt(sar)(3-but)Cl, as revealed by the methyl region of the ^{1}H spectrum of each. Though very little stereoselectivity is evident in the distribution of trans isomers, two of the cis isomers are clearly dominant over two lesser species. The ^{195}Pt spectra were often used to corroborate assignments of stereochemistry and to monitor the conversion of trans to cis species in aqueous reaction mixtures.

Several generalizations can be derived from a systematic comparison of the NMR data for the 24 combinations (48 potentially NMR-distinguishable isomers) of trans and cis isomers of the three olefins with four amino acids. First of all, (1) proton and carbon-13 shifts of all olefinic protons and carbons in the

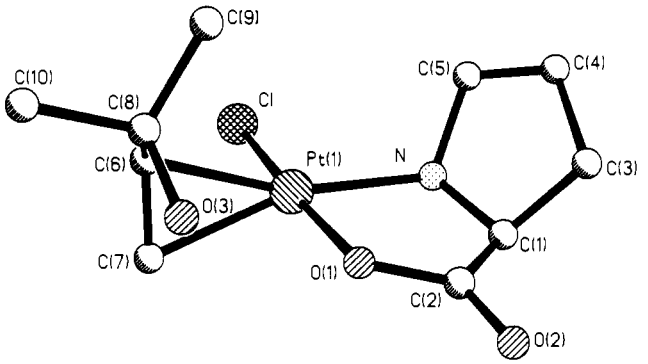

Figure 4. Structure of *trans*(*N,olefin*)-Pt(*S*-pro)(*R*-2-mb)Cl (**10**).

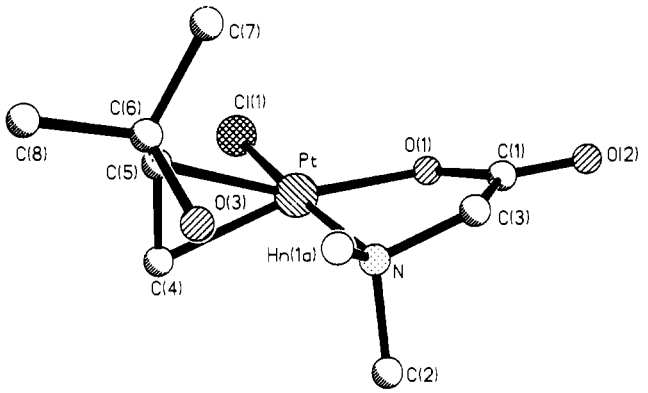

Figure 5. Structure of *cis*(*N,olefin*)-Pt(sar)(2-mb)Cl (**11**). The *S*-N_1,*R*-C_1 enantiomer of the racemic pair is shown.

complexes are substantially less positive (nuclei more shielded) than corresponding shifts of free olefins. The coordination shift amounts to 0.5–1.0 ppm for protons and 30–40 ppm for carbon-13. More importantly, (2) for three key nuclei, the shifts of the cis isomers generally lie at less positive (more shielded) values than those of the corresponding trans isomers. The size of the difference also depends on the amino acid, but the differences are about 0.5 ppm for protons H_t and H_c (less for H_x), 10 ppm for the olefinic carbons, and 200–400 ppm for ^{195}Pt. In addition, (3) the spin-coupling constants between Pt and olefinic protons ($^2J_{Pt-H}$) and between Pt and olefinic carbons ($^1J_{Pt-C}$) are also larger for the cis isomer than for the corresponding trans isomer. The difference in both cases amounts to 10–15%: from about 60 to about 70 Hz for $^2J_{Pt-H}$ and from about 170 to about 200 Hz for $^1J_{Pt-C}$.

In addition to these large, systematic, and diagnostically useful trends in NMR parameters, additional, more subtle patterns evident in the spectra include the following: (4) For all 2-mb complexes, the proton chemical shift difference between the two methyl groups is about the same (0.3 ppm), but the carbon-13 shift difference between the two methyl groups is somewhat greater for cis than for trans isomers. In addition, the $^3J_{Pt-C}$ coupling constants for the two nonequivalent methyls differ systematically, with the more shielded carbon being universally less strongly coupled to ^{195}Pt (10–20 vs 30–50 Hz). (5) The relative chemical shifts of olefin methylene protons H_c and H_t are quite similar for all three olefins, so H_c is sometimes more shielded than H_t (as it is in the free olefins) and sometimes less shielded. The two protons also have different line widths. Both of these properties are related to the relative population of rotamers for rotation about the Pt–olefin bond, which we are currently exploring further in variable-temperature experiments. (6) The effect on the chemical shifts of the olefinic carbons of replacing the two α-protons of allyl alcohol with methyl groups is in agreement with well-documented methyl substitution effects on carbon chemical shifts. Thus, C_1 carbon (terminal olefin) shifts are not as much affected by the substitution at C_3 as the C_2 and C_3 carbon shifts, but all three move systematically toward more positive values with increased methyl substitution at C_3. The methyl substitution effect on C_1 for this series is enough smaller than the cis vs trans isomer

Table III. Atomic Coordinates ($\times 10^4$) and Equivalent Isotropic Displacement Parameters ($Å^2 \times 10^3$) in Pt(*S*-pro)(2-mb)Cl (**10**)

	x	*y*	*z*	*U*(eq)[a]
Pt	7299 (1)	338 (1)	3629 (1)	31 (1)
Cl	7572 (10)	2574 (5)	3764 (4)	74 (2)
O(1)	7186 (19)	−1628 (13)	3447 (7)	42 (3)
O(2)	8246 (29)	−3230 (14)	2734 (9)	57 (5)
O(3)	4327 (25)	−2021 (13)	4422 (9)	52 (5)
N	8318 (24)	399 (14)	2616 (8)	37 (4)
C(1)	8687 (30)	−995 (19)	2348 (9)	39 (5)
C(2)	8022 (26)	−2047 (18)	2863 (9)	37 (5)
C(3)	7650 (47)	−1051 (27)	1650 (12)	70 (10)
C(5)	6839 (50)	1014 (24)	2100 (14)	69 (9)
C(6)	5318 (27)	314 (16)	4514 (11)	42 (5)
C(7)	7136 (40)	15 (30)	4737 (10)	69 (9)
C(8)	3691 (27)	−645 (20)	4434 (12)	46 (6)
C(9)	2446 (30)	−445 (20)	3833 (16)	69 (8)
C(10)	2544 (35)	−584 (26)	5128 (14)	72 (9)
C(4)	7088 (124)	425 (68)	1489 (38)	95 (23)
C(4′)	6008 (108)	27 (61)	1752 (34)	74 (15)

[a] Equivalent isotropic *U* defined as one-third of the trace of the orthogonalized U_{ij} tensor.

Table IV. Atomic Coordinates ($\times 10^4$) and Equivalent Isotropic Displacement Parameters ($Å^2 \times 10^3$) in Pt(sar)(2-mb)Cl (**11**)

	x	*y*	*z*	*U*(eq)[a]
Pt	563 (1)	5092 (1)	2774 (1)	28 (1)
Cl	844 (5)	6540 (3)	3486 (3)	47 (1)
N	279 (12)	3904 (8)	2023 (7)	30 (4)
O(1)	1022 (11)	5716 (7)	1660 (7)	36 (3)
O(2)	1595 (14)	5324 (8)	345 (7)	57 (4)
O(3)	720 (11)	2746 (6)	3367 (7)	47 (4)
C(1)	1252 (16)	5094 (11)	1054 (9)	37 (5)
C(6)	1487 (16)	3321 (9)	3904 (10)	34 (5)
C(4)	−403 (16)	4520 (12)	3840 (10)	39 (5)
C(5)	866 (15)	4337 (10)	3937 (10)	34 (5)
C(2)	−1059 (18)	3802 (13)	1771 (13)	55 (7)
C(7)	2800 (18)	3389 (12)	3580 (14)	66 (8)
C(8)	1479 (22)	2916 (11)	4770 (11)	63 (8)
C(3)	1055 (20)	4020 (11)	1270 (10)	48 (6)

[a] Equivalent isotropic *U* defined as one-third of the trace of the orthogonalized U_{ij} tensor.

Table V. Atomic Coordinates ($\times 10^4$) and Equivalent Isotropic Displacement Parameters ($Å^2 \times 10^3$) in Pt(sar)(Me_2SO)Cl (**12**)

	x	*y*	*z*	*U*(eq)[a]
Pt	3106 (1)	5969 (1)	1637 (1)	22 (1)
Cl	1907 (3)	5944 (2)	439 (2)	40 (1)
S	4623 (2)	6958 (2)	1081 (2)	26 (1)
O(1)	5716 (7)	7235 (7)	1623 (4)	37 (3)
O(3)	1194 (9)	4444 (7)	3442 (5)	42 (3)
O(2)	1694 (6)	5125 (7)	2229 (5)	33 (2)
N	4014 (8)	5843 (8)	2759 (6)	30 (3)
C(4)	3404 (11)	4942 (10)	3175 (7)	35 (3)
C(3)	1973 (10)	4818 (9)	2964 (6)	26 (3)
C(1)	3934 (11)	8190 (8)	731 (7)	34 (3)
C(2)	5238 (11)	6431 (10)	163 (7)	37 (4)
C(5)	3938 (13)	6895 (10)	3230 (8)	44 (4)

[a] Equivalent isotropic *U* defined as one-third of the trace of the orthogonalized U_{ij} tensor.

difference that the chemical shift of C_1 is a reliable indicator of cis (69 ± 3 ppm) vs trans (58 ± 3 ppm) geometry of any of the complexes in the series.

X-ray Structures of 2-mb Complexes. The X-ray structures of the less soluble isomer of *trans*-Pt(*S*-pro)(2-mb)Cl (**10**) and of one of the enantiomers of the single dominant diastereomer of *cis*-Pt(sar)(2-mb)Cl (**11**) are shown in Figures 4 and 5. Atomic coordinates for the two compounds are listed in Tables III and IV; bond lengths/angles, in Tables VI–IX. The absolute configuration of chiral centers in **10** is revealed to be *trans*-Pt(*S*-C_1,*S*-N_1-Pro)(*R*-2-mb)Cl. By contrast, crystals of **11** consist of a racemic mixture of both *cis*-Pt(*S*-sar)(*R*-2-mb)Cl (shown in Figure 5) and an equal population of *cis*-Pt(*R*-sar)(*S*-2-mb)Cl.

Table VI. Bond Lengths (Å) in Pt(*S*-pro)(2-mb)Cl (**10**)

Pt–Cl	2.253 (5)	C(1)–C(3)	1.515 (31)
Pt–O	1.992 (13)	C(3)–C(4)	1.553 (75)
Pt–N	2.059 (16)	C(3)–C(4′)	1.581 (75)
Pt–C(6)	2.178 (20)	C(5)–C(4)	1.316 (77)
Pt–C(7)	2.139 (19)	C(5)–C(4′)	1.320 (72)
O(1)–C(2)	1.324 (22)	C(6)–C(7)	1.366 (33)
O(2)–C(2)	1.215 (23)	C(6)–C(8)	1.489 (26)
O(3)–C(8)	1.442 (24)	C(8)–C(9)	1.449 (35)
N–C(1)	1.502 (24)	C(8)–C(10)	1.546 (35)
N–C(5)	1.549 (34)	C(4)–C(4′)	0.986 (107)
C(1)–C(2)	1.509 (26)		

Table VII. Bond Angles (deg) in Pt(*S*-pro)(2-mb)Cl (**10**)

Cl–Pt–O(1)	175.7 (4)	N–C(5)–C(4)	107.3 (40)
Cl–Pt–N	92.8 (4)	N–C(5)–C(4′)	108.3 (33)
O(1)–Pt–N	83.1 (6)	C(4)–C(5)–C(4′)	43.9 (46)
Cl–Pt–C(6)	88.6 (5)	Pt–C(6)–C(7)	70.0 (12)
O(1)–Pt–C(6)	95.7 (6)	Pt–C(6)–C(8)	114.1 (14)
N–Pt–C(6)	160.9 (7)	C(7)–C(6)–C(8)	126.5 (19)
Cl(1)–Pt–C(7)	92.3 (8)	Pt–C(7)–C(6)	73.1 (12)
O(1)–Pt–C(7)	91.3 (9)	O(3)–C(8)–C(6)	112.3 (16)
N–Pt–C(7)	161.6 (9)	O(3)–C(8)–C(9)	107.6 (17)
C(6)–Pt–C(7)	36.9 (9)	C(6)–C(8)–C(9)	116.6 (18)
Pt–O(1)–C(2)	116.1 (11)	O(3)–C(8)–C(10)	102.0 (17)
Pt–N–C(1)	110.5 (11)	O(6)–C(8)–C(10)	106.2 (18)
Pt–N–C(5)	112.2 (14)	C(9)–C(8)–C(10)	111.2 (18)
C(1)–N–C(5)	105.3 (15)	C(3)–C(4)–C(5)	106.3 (48)
N–C(1)–C(2)	111.7 (14)	C(3)–C(4)–C(4′)	73.2 (56)
N–C(1)–C(3)	104.6 (17)	C(5)–C(4)–C(4′)	68.2 (58)
C(2)–C(1)–C(3)	113.6 (18)	C(3)–C(4′)–C(5)	104.6 (50)
O(1)–C(2)–O(2)	122.2 (17)	C(3)–C(4′)–C(4)	70.2 (60)
O(1)–C(2)–C(1)	117.5 (16)	C(5)–C(4′)–C(4)	67.8 (58)
O(2)–C(2)–C(1)	120.3 (17)	Cl–Pt–X[a]	90.6
C(1)–C(3)–C(4)	104.9 (32)	O(1)–Pt–X	93.4
C(1)–C(3)–C(4′)	102.1 (29)	N–Pt–X	176.1
C(4)–C(3)–C(4′)	36.7 (39)		

[a] X is the midpoint of C(6) and C(7).

Table VIII. Bond Lengths (Å) in Pt(sar)(2-mb)Cl (**11**)

Pt–Cl	2.302 (4)	O(2)–C(1)	1.227 (19)
Pt–N	2.039 (11)	O(3)–C(6)	1.422 (19)
Pt–O(1)	2.027 (10)	C(1)–C(3)	1.523 (21)
Pt–C(4)	2.135 (16)	C(6)–C(5)	1.540 (19)
Pt–C(5)	2.144 (15)	C(6)–C(7)	1.500 (26)
N–C(2)	1.493 (24)	C(6)–C(8)	1.485 (23)
N–C(3)	1.466 (21)	C(4)–C(5)	1.391 (23)
O(1)–C(1)	1.308 (18)	Pt–X[a]	1.995

[a] X is the midpoint of C(4) and C(5).

Table IX. Bond Angles (deg) in Pt(sar)(2-mb)Cl (**11**)

Cl–Pt–N	173.4 (3)	O(2)–C(1)–C(3)	119.7 (13)
Cl–Pt–O(1)	92.1 (3)	O(3)–C(6)–C(5)	105.7 (12)
N–Pt–O(1)	81.9 (4)	O(3)–C(6)–C(7)	111.7 (14)
Cl–Pt–C(4)	89.3 (4)	C(5)–C(6)–C(7)	111.1 (12)
N–Pt–C(4)	95.8 (5)	O(3)–C(6)–C(8)	110.3 (12)
O(1)–Pt–C(4)	165.0 (6)	C(5)–C(6)–C(8)	107.6 (13)
Cl–Pt–C(5)	88.2 (4)	C(7)–C(6)–C(8)	110.2 (16)
N–Pt–C(5)	98.4 (5)	Pt–C(4)–C(5)	71.4 (9)
O(1)–Pt–C(5)	157.0 (6)	Pt–C(5)–C(6)	118.0 (10)
C(4)–Pt–C(5)	37.9 (6)	Pt–C(5)–C(4)	70.7 (9)
Pt–N–C(2)	112.0 (10)	C(6)–C(5)–C(4)	125.4 (13)
Pt–N–C(3)	107.9 (9)	N–C(3)–C(1)	111.5 (12)
C(2)–N–C(3)	109.5 (13)	Cl(1)–Pt–X[a]	89.2
Pt–O(1)–C(1)	114.6 (9)	N–Pt–X	97.1
O(1)–C(1)–O(2)	124.6 (13)	O(1)–Pt–X	175.9
O(1)–C(1)–C(3)	115.7 (13)		

[a] X is the midpoint of C(4) and C(5).

In both of these structures, the observed orientation of the $C(CH_3)_2OH$ substituent about the Pt–olefin bond is the one in which the substituent is oriented away from the chloride, which is cis to the olefin. In addition, in both structures, the rotational orientation of the $C(CH_3)_2OH$ moiety about the C–C bond places OH relatively close to O or N (of the amino acid), which lies cis

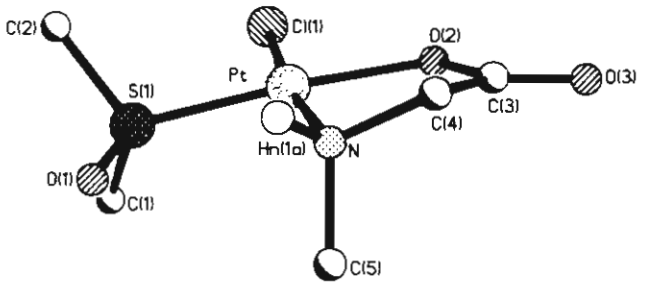

Figure 6. Structure of *cis*(*N*,*S*)-Pt(sar)(Me_2SO)Cl (**12**).

Table X. Bond Lengths (Å) in Pt(sar)(Me_2SO)Cl (**12**)

Pt–Cl	2.304 (3)	S–C(2)	1.746 (11)
Pt–S	2.180 (3)	O(3)–C(3)	1.209 (13)
Pt–O(2)	2.033 (7)	O(2)–C(3)	1.283 (13)
Pt–N	2.052 (9)	N–C(4)	1.448 (15)
S–O(1)	1.468 (8)	N–C(5)	1.515 (16)
S–C(1)	1.777 (11)	C(4)–C(3)	1.520 (15)

Table XI. Bond Angles (deg) in Pt(sar)(Me_2SO)Cl (**12**)

Cl–Pt–S	92.4 (1)	O(1)–S–C(2)	108.7 (5)
Cl–Pt–O(2)	90.5 (2)	C(1)–S–C(2)	101.1 (5)
S–Pt–O(2)	175.7 (2)	Pt–O(2)–C(3)	115.6 (6)
Cl–Pt–N	172.6 (3)	Pt–N–C(4)	106.0 (7)
S–Pt–N	94.8 (3)	Pt–N–C(5)	111.0 (7)
O(2)–Pt–N	82.3 (3)	C(4)–N–C(5)	114.0 (9)
Pt–S–O(1)	115.6 (3)	N–C(4)–C(3)	113.1 (9)
Pt–S–C(1)	109.3 (4)	O(3)–C(3)–O(2)	124.2 (10)
O(1)–S–C(1)	107.3 (5)	O(3)–C(3)–C(4)	122.5 (10)
Pt–S–C(2)	113.7 (4)	O(2)–C(3)–C(4)	113.3 (9)

to the olefin. This orientation leaves one methyl group anti and the other methyl group and OH gauche to Pt in the Pt–C–C–X portion of the coordinated 2-mb. The structure of *cis*-Pt(*S*-sar)(*R*-2-mb)Cl also minimizes the expected unfavorable steric interaction between the $C(CH_3)_2OH$ moiety of the olefin and $N–CH_3$ of coordinated sarcosine by placing the two groups on opposite sides of the coordination plane and $N–CH_3$ in an extreme axial orientation on the puckered five-membered glycinate chelate ring. The same glycinate ring puckering enables *cis*(*N*,*S*)-Pt(sar)(Me_2SO)Cl (**12**), whose structure (of the enantiomer with the *S* configuration at N depicted) is shown in Figure 6 (data in Tables V, X, and XI), to mimimize unfavorable steric interaction between $N–CH_3$ and coordinated dimethyl sulfoxide, which occupies the adjacent cis position.

A comparison of glycinate ring geometry in the solid state and solution NMR data for *cis*-Pt(*S*-sar)(*R*-2-mb)Cl and *cis*-Pt(*S*-sar)(Me_2SO)Cl shows that the puckered glycinate ring conformation of the chelated sarcosine in the solid state persists in solution. Table XII lists Pt–N–C–H dihedral angles for the solid (based on calculated H positions) and 3-bond vicinal ^{195}Pt coupling constants and proton chemical shifts for solutions of the two sarcosine complexes. The observed $^3J_{Pt-H}$ values correspond closely to values expected on the basis of a Karplus-type $\cos^2\phi$ dependence with J_{max} = 90 Hz.[15] Furthermore, the chemical shift difference between methylene protons (~0.70 ppm) is significantly greater than observed for any trans(N,olefin) isomers we have examined. To the extent that the solid-state structures for 2-mb complexes persist in solution, these structures permit assignment of the stereochemistry of the rest of the isomers revealed by ^1H, ^{13}C, and ^{195}Pt NMR spectra of the series.

Stereochemistry and Relative Populations of Diastereomers. The notation used to denote stereochemical configurations and the relative populations of isomers of the 16 diastereomeric compounds included in this study is given in Table XIII. The basis of the isomer assignments is outlined below. Relative populations were calculated from integration of appropriate portions of the proton

Table XII. Solution NMR Parameters and Solid-State Pt–N–C–H Dihedral Angles ϕ for Sarcosine Methylene Protons[a]

complex	ϕ_A	$^3J_{Pt-H_A}$	δ_A	ϕ_B	$^3J_{Pt-H_B}$	δ_B	$\Delta\delta$
cis-Pt(*S*-sar)(*R*-2-mb)Cl	154.1	65	3.260	89.1	<10	3.935	0.675
cis-Pt(sar)-(Me_2SO)Cl	153.5	73	3.419	89.2	<10	4.123	0.704

[a] ϕ in deg, J in Hz, and δ in ppm.

NMR spectrum, but similar ratios were reflected in the relative intensities of corresponding peaks in the ^{13}C or ^{195}Pt spectra.

The relative stereochemistry of isomers can be assigned unambiguously to *trans*-Pt(*S*-pro)(2-mb)Cl, and to *cis*-Pt(sar)(2-mb)Cl, on the basis of the X-ray crystal structures. For *trans*-Pt(*S*-pro)(2-mb)Cl, the isolated diastereomer is also the one that predominates (0.54 vs. 0.46) at equilibrium after equilibration in the presence of free 2-mb.[9] For *trans*-Pt(*S*-pro)(allOH)Cl, the assignment of stereochemistry to the two diastereomers (with a slight preference for the *trans*-Pt(*S*-pro)(*R*-allOH)Cl isomer) is based on the close similarity in chemical shift patterns for olefinic protons and carbons between corresponding allOH and 2-mb complexes. Similarly, the strongly preferred (0.83/0.17) isomer of *cis*-Pt(sar)(allOH)Cl is assumed to be the *cis*-Pt(*S*-sar)(*R*-allOH(Cl form, parallel to the single isomer (98%) of *cis*-Pt(*S*-sar)(*R*-2-mb)Cl, which is evident in equilibrated solutions of that compound. This assignment is also supported by the large chemical shift difference between sarcosine methylene protons (0.77 ppm) and $^3J_{PtH}$ for the more shielded methylene proton (65 Hz) of the dominant isomer, which corresponds closely to values noted in Table XII for the dominant *cis*-Pt(*S*-sar)(*R*-2-mb) isomer.

The almost complete lack of stereoselectivity of coordination of 3-but (Figure 1) in the four complexes of 3-but with cis and trans isomers of achiral glycine and α-aminoisobutyric acid makes the assignment of stereochemistry for those species less significant, but the assignments given in Table XIII are based on the following arguments. Selective decoupling experiments and relative intensities of peaks have permitted complete separation of the proton and carbon-13 spectra of the two isomers in equilibrium mixtures for each of the four pairs. The large differences in chemical shifts of α-H and of $^3J_{Pt-C}$ for α-methyl of 3-but can be invoked to support specific isomer assignments, if one assumes a particular preferred rotational orientation of the $CH(CH_3)(OH)$ fragment about the $C_2–C_3$ bond and of the olefin about the Pt–olefin bond. The X-ray structures of *trans*-Pt(*S*-pro)(*R*-2-mb)Cl, *cis*-Pt(*S*-sar)(*R*-2-mb)Cl, and of both *cis*- and *trans*-Pt(aba)(2-mb)Cl[16] show that the $C(CH_3)_2(OH)$ fragment is oriented away from the Cl atom and that the OH is oriented toward the coordinated O (trans) or N (cis) of the amino acid in every case in the solid state. If that orientation is also preferred in solution for the $CH(CH_3)(OH)$ fragment of the 3-but complexes, the isomer that has the larger $^3J_{Pt-C}$ coupling (isomer 1 in Figure 1) would be assigned the stereochemistry *S*-C_2,*S*-C_3 (or *R*-C_2,*R*-C_3), since CH_3 would be more nearly trans to Pt in the Pt–C–C–CH_3 fragment, as shown in **13a**. Support for this argument is provided by comparing ^{13}C

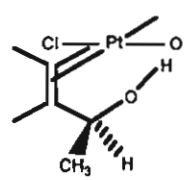

13a
S-C_2, S-C_3

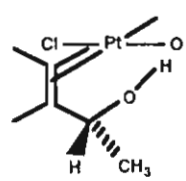

13b
R-C_2, S-C_3

shifts and $^3J_{Pt-C}$ values for 2-mb and 3-but complexes. In the 2-mb complexes, the lower frequency methyl carbon is always the one which is less strongly coupled to platinum (Figure 2); and, in the

(15) As suggested originally by: Erickson, L. E.; Erickson, M. D.; Smith, B. L. *Inorg. Chem.* **1973**, *12*, 412.

(16) Unpublished structures determined by L. Erickson and K. Haller, University of Wisconsin, 1983.

Table XIII. Equilibrium Populations of Diastereomers

compd	isomer stereochem[a]	fractional population ratios
trans-Pt(gly)(3-but)Cl	**RR*/**SR* = **SS*/**RS*	0.79 ± 0.05
cis-Pt(gly)(3-but)Cl	**RR*/**SR* = **SS*/**RS*	1.00 ± 0.05
trans-Pt(aba)(3-but)Cl	**RR*/**SR* = **SS*/**RS*	0.79 ± 0.05
cis-Pt(aba)(3-but)Cl	**RR*/**SR* = **SS*/**RS*	1.00 ± 0.05
trans-Pt(sar)(allOH)Cl	*S*R*/*S*S* = *R*S*/*R*R*	1.00 ± 0.05
cis-Pt(sar)(allOH)Cl	*S*R*/*S*S* = *R*S*/*R*R*	6.00 ± 0.10
trans-Pt(sar)(2-mb)Cl	*S*R*/*S*S* = *R*S*/*R*R*	0.92 or 1.08 ± 0.05
cis-Pt(sar)(2-mb)Cl	*S*R*/*S*S* = *R*S*/*R*R*	>40
trans-Pt(sar)(3-but)Cl	*SRR*/*SSR*/*SRS*/*SSS*[b]	~0.25/0.25/0.25/0.25
cis-Pt(sar)(3-but)Cl	*SRR*/*SSR*/*SRS*/*SSS*[b]	0.40/0.46/0.06/0.08
	(*SRR* + *SSR*)/(*RRR* + *RSR*)	6.1 ± 0.10
trans-Pt(*S*-pro)(allOH)Cl	*S*R*/*S*S*	1.08 ± 0.05
cis-Pt(*S*-pro)(allOH)Cl	*S*R*/*S*S*	>5
trans-Pt(*S*-pro)(2-mb)Cl	*S*R*/*S*S*	1.27 ± 0.05
cis-Pt(*S*-pro)(2-mb)Cl	*S*R*/*S*S*	>30
trans-Pt(*S*-pro)(3-but)Cl	*SRR*/*SSR*/*SRS*/*SSS*	~0.25/0.25/0.25/0.25
cis-Pt(*S*-pro)(3-but)Cl	*SRR*/*SSR*/*SRS*/*SSS*	~0.4/0.4/0.1/0.1
	(*SRR* + *SSR*)/(*SRS* + *SSS*)	>4

[a] As illustrated below, the stereochemistry at the three chiral sites (1) amino acid nitrogen, (2) α-carbon of 3-but, and (3) olefinic carbon bound to Pt, respectively, is denoted by *SSS* if all three chiral centers have the *S* configuration and by **RR*, *RS**, etc. if the first or third center is not chiral. For (*S*)-proline chelate species, the configuration at both N_1 and the α-C is necessarily *S*.

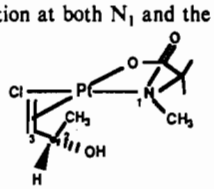

cis(N,3-but)-Pt(S-sar)(S,S-3-but)Cl = SSS

[b] *SRR*/*SSR*/*SRS*/*SSS* = *RSS*/*RRS*/*RSR*/*RRR*.

3-but diastereomer pairs (Figure 3), the one which has the lower frequency methyl signal is also the one which is less strongly coupled to platinum.

The stereoselectivity of olefin coordination in 3-but complexes of sarcosine or proline corresponds quite closely to the expectations of a combination of the intraligand and interligand effects that have been noted to this point. For *trans*- and *cis*-Pt(sar)(3-but)Cl and Pt(*S*-pro)(3-but)Cl, four NMR-distinguishable diastereomers can be expected on the basis of the three chiral centers in each complex. Since little selectivity is observed in 3-but complexes with achiral amino acids or in trans isomers of sar or pro with allOH or 2-mb, the appearance of four species at essentially equal concentrations for *trans*-Pt(sar)(3-but)Cl (Figure 2) and *trans*-Pt(*S*-pro)(3-but)Cl is not surprising. By contrast, the asymmetry in equilibrium concentrations of the four isomers of *cis*-Pt(sar)(3-but)Cl (Figure 2) can be accounted for readily by a significant interligand interaction between the nitrogen chiral center of sarcosine and the olefin chiral center at C_3, coupled with almost no intraligand interaction between chiral centers at C_2 and C_3 of 3-but. The two major species can be identified as the counterparts of the dominant species in *cis*-Pt(sar)(2-mb)Cl, with the same stereochemistry as the dominant 2-mb species at C_3 of the olefin and at N-methyl of sarcosine; i.e., as *SRR* and *SSR*. The two major species have opposite configurations at C_2, but that intraligand difference has little effect on the energy or relative concentration at equilibrium. Similarly, the two lesser species correspond to the lower concentration isomer of *cis*-Pt(sar)(allOH)Cl and would be expected again to have the corresponding stereochemistry at the chiral carbon of the olefin (*S*) and at N-methyl of sarcosine (*S*). Like the dominant pair, the two lesser species differ only in stereochemistry at C_2 of 3-but, so they are denoted *SRS* and *SSS*. In each pair, the more shielded and less intense CCH_3 doublet can be identified as the *SRR* or *SSS* isomer. In any case, the ratio of the sum of the concentrations of the dominant pair to the lesser pair (6.1 ± 0.1) is similar to the ratio observed for the two diastereomers of *cis*-Pt(sar)(allOH)Cl (6.0 ± 0.1). The lack of an N–CH_3 signal and extensive overlap of olefin CH_3 and proline CH_2 signals in the proton NMR spectrum make a quantitative assessment of the isomer ratios for *cis*-Pt(*S*-pro)(3-but)Cl less accurate than for the *cis*-Pt(sar)(3-but)Cl species, but two diastereomers—presumably *SSR* and *SRR*, on the basis of the similarities in chemical shifts of C–CH_3 signals—account for >80% of the C-methyl absorption.

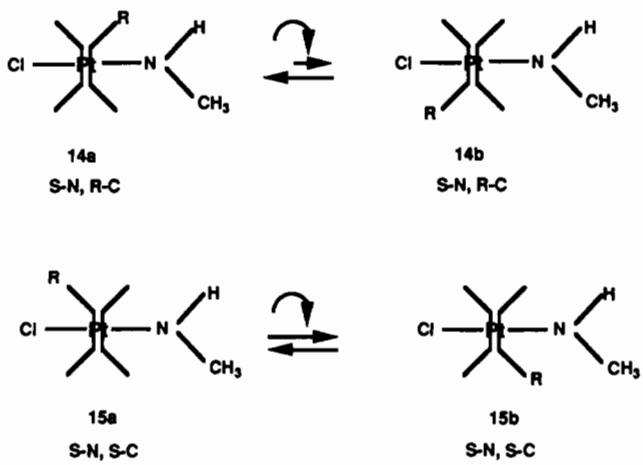

Figure 7. Rotamers of the two diastereomers of *cis*(*N,olefin*)-Pt(*S*-sar)(CH_2=CHR)Cl.

Discussion

Steric Interactions in Cis(N,Olefin) Sarcosine and Proline Complexes. The exceptionally high degree of stereoselectivity of *cis*-Pt(sar)(olefin)Cl and *cis*-Pt(*S*-pro)(olefin)Cl species in this series, which contrasts sharply to the general lack of significant stereoselectivity for trans isomers (even with chiral amino acids), warrants closer examination. The cis(N,olefin) isomer of Pt(sar)(olefin)Cl, for which the quantitative data are more reliable, is much more stereoselective than the trans isomer and 2-mb is more stereoselective than 3-but or allOH. This indicates that steric interaction between the pendant olefin moiety and N-methyl of sarcosine is the most important interaction in these species. The two rotamers of the two diastereomers of *cis*-Pt(*S*-sar)(CH_2=CHR)Cl with a prochiral olefin are shown in Figure 7, as viewed from the olefin side parallel to the coordination plane. For each isomer, the R group can be oriented either toward the Cl atom or toward the coordinated nitrogen of the amino acid moiety. The barrier to rotation about the Pt–olefin bond is sufficiently low to permit rapid interconversion of rotamers **14a** and **14b** or **15a** and **15b** at room temperature. Variable-temperature proton NMR experiments in progress on *cis*-Pt(aba)(2-mb)Cl and *cis*-Pt(gly)(2-mb)Cl indicate that the coordinated 2-mb strong

(~10/1) one rotamer, presumably the one for which $C(CH_3)_2OH$ is oriented away from the cis Cl, at room temperature. For *cis*-Pt(*S*-sar)(*S*-2-mb)Cl, the choice is between an unfavorable R–Cl interaction (**15a**) and an unfavorable R–CH_3 interaction (**15b**). However, with **14a**—the stable rotamer in the solid state—available to *cis*-Pt(*S*-sar)(R-2-mb)Cl, the *S*-N,*R*-C isomer prevails by a margin of at least 40/1 over the *S*-N,*S*-C isomer.

Conformation of the CR_1R_2OH Fragment. In the preceding discussion, we have ignored the effect of rotation about the C_2–C_3 axis on the observed isomer distributions. For both trans and cis isomers of 2-mb complexes, the very different chemical shifts (both proton and carbon-13) of the two methyl groups indicate that they have substantially different average environments, with one methyl oriented approximately anti to the central platinum. This conclusion is again supported by the X-ray structure data on the solid. As shown in Figures 4 and 5, for both trans and cis isomers, the olefin side chain is oriented toward the amino acid oxygen or nitrogen with the olefin OH oriented toward the amino acid oxygen (trans isomer) or nitrogen (cis isomer), possibly supported by intramolecular hydrogen bonding.[17] Similarly, for the 3-but diastereomers of *cis*-Pt(gly)(3-but)Cl, NMR data show that one of the two equally stable isomers has its methyl group oriented preferentially anti to the central Pt. These isomers have little difference in energy because there is no bulky group attached to the nitrogen and intraligand effects for coordinated 3-but are negligible. However, for the four *cis*-Pt(sar)(3-but)Cl isomers, two isomers allow the side chain to avoid N-methyl, but the other two require either an unfavorable R–Cl or R–CH_3 interaction. In either case, the interaction can be made less unfavorable by orienting C–H toward N–CH_3. This probably accounts for the higher equilibrium concentration of these two minor isomers for 3-but relative to the single minor isomer of the corresponding 2-mb species.

Finally, for allyl alcohol complexes, with no methyl groups attached to the α-carbon, an even smaller ratio of isomers might be expected. In fact, the ratio (6.0) is not significantly different from the 6.1 of the 3-but analogues. The differences in sarcosine proton shifts and in $^3J_{Pt-H}$ coupling constants between isomers suggest that the same changes in rotamer distributions that account for the 3-but data are operative here too. Like the 3-but species, the lesser (*S*,*S*) species has the more shielded N–CH_3 protons, probably because of the effect of the CH_2OH group of the adjacent olefin. However, the interaction between N–CH_3 and CH_2OH of allOH is less than the interaction between N–CH_3 and the $C(CH_3)_2OH$ moiety of 2-mb, so a significant concentration of *SS* isomer can exist in equilibrium with the preferred *SR* isomer.

Other Aspects of the Structures of 10–12. Bond lengths and angles reported here for **10–12** are generally typical of values reported in the literature for similar complexes of Pt(II). However, several specific features should be noted. The Pt–X bond lengths reflect both the identity and the geometry of the other ligands in the coordination sphere, so the bond lengths of **10** and **11** are quite close to those reported for *trans*-Pt(β-alanine)(ethylene)Cl[12] and other neutral cis- or trans(N,olefin) species containing one or two chlorides.[18-23] The differences in Pt–X bond lengths between **10** and **11**, which might be attributed to the trans vs cis geometry around the central Pt, are barely evident at the 3σ level. However, the same pattern, longer Pt–Cl and shorter Pt–N and Pt–olefin distances, is seen in data for the cis and trans isomers of Pt(aba)(2-mb)Cl.[16] The shorter Pt–olefin carbon bonds for cis isomers could be expected on the basis of the 10–20% larger NMR coupling constants between Pt and olefinic carbons observed for cis isomers with a given amino acid–olefin combination. Similar systematic differences in NMR coupling constants have been noted for analogous cis and trans isomers of mixed sulfoxide–amino acid complexes.[23] For both **10** and **11**, the C–C bond of the chiral olefin is tilted with respect to the perpendicular of the mean plane defined by the Pt–N–O–Cl atoms, but the midpoint of the bond lies essentially in that plane. In each case the tilt (11.2° for **10** and 2.7° for **11**) relieves crowding between the $C(CH_3)_2OH$ moiety and substituents on the amino acid fragment by moving the $C(CH_3)_2OH$ moiety away from the coordination plane.[16,18,19]

The Pt–X bond lengths of **12** lie in the range expected on the basis of data for similar sulfoxide complexes like *trans*-PtCl(Me_2SO)$(NH_3)_2^+$,[25] *cis*-$PtCl_2(Me_2SO)NH_3$,[26] and PtCl(en)$(Me_2SO)^+$,[27] and the two sarcosine complexes, **11** and **12**, which differ only in having the sulfoxide and olefin interchanged, have very similar structural properties for the rest of the molecule. We have already noted the similarities in glycinate ring conformations (Table XII); the Pt–N and Pt–Cl bonds are also essentially identical. The slightly longer Pt–O bond lengths (Å) of **12** (2.033) compared to **11** (1.998) would be consistent with the greater trans influence of dimethyl sulfoxide relative to 2-mb.[28] A similar difference is evident in the trans Pt–Cl bond lengths of Pt(ethylene)Cl_3^- (2.357)[29] and Pt(Me_2SO)Cl_3^- (2.327).[30] However, the uncertainties in all four of these bond lengths make such comparisons tenuous. Both the sulfur-coordinated sulfoxide of **12** and the coordinated 2-mb of **11** are oriented so as to permit intramolecular hydrogen-bond formation betwen N–H and an oxygen atom, the oxygen atom of the sulfoxide or O–H of 2-mb. However, the greater distance between the N–H proton (at its calculated location) and the sulfoxide oxygen (2.70) compared to the 2-mb hydroxyl oxygen (1.84) suggests a substantially weaker hydrogen bond for the former.

Implications of Stereoselective Olefin Binding by N-Chiral Complexes. The degree of stereoselectivity of olefin coordination of 2-mb in *cis*-Pt(sar)(2-mb)Cl and *cis*-Pt(*S*-pro)(2-mb)Cl is truly exceptional. As Gladysz and co-workers noted in their report of diastereomer ratios of (95–98)/(5–2) for [(η^5-C_5H_5)Re(NO)$(PPh_3)(CH_2{=}CHR)]BF_4$ (for R = CH_3, C_3H_7, CH_2–C_6H_5), "no homogenous binding agent exists that efficiently and predictably discriminates between the enantiofaces of simple monosubstituted alkenes $H_2C{=}CHR$",[31] though some stereoselectivity has also been reported for the corresponding Fe complex with propene.[32]

The large stereoselectivity of olefin binding found here for cis(N,olefin) complexes has potential synthetic applications, since any reagent that reacts stereoselectively with a metal-bound prochiral olefin would be expected to yield a specific isomeric product. Possible reactions include hydrogenation, epoxidation, and polymerization.[1] However, as the extensive work on the stereochemistry of chiral phosphine–rhodium catalysis[33] of olefin hydrogenation and similar studies of the effect of chiral diamine ligands on the isomer distribution of dihydroxylation of olefins by OsO_4[34] have established, the stereochemistry of the product of a reaction that involves a coordinated prochiral olefin can be

(17) By contrast, the CH_2OH moiety of the coordinated allyl alcohol in *cis*-[$PtCl_2(PMe_2Ph)$(allOH)] is oriented toward the cis chloride.[8]
(18) Benedetti, L.; Corradini, P.; Pedone, C. *J. Organomet. Chem.* **1969**, *18*, 203.
(19) Pedone, C.; Benedetti, E. *J. Organomet. Chem.* **1971**, *29*, 443.
(20) Caruso, F.; Spagna, R.; Zambonelli, L. *Inorg. Chim. Acta* **1973**, *32*, 123.
(21) Deese, W. C.; Johnson, D. A.; Cordes, A. W. *Inorg. Chem.* **1981**, *20*, 1519.
(22) Johnson, D. A.; Deese, W. C.; Cordes, A. W. *Acta Crystallogr.* **1981**, *B37*, 2220.
(23) Kops, R. T.; van Aken, E.; Schlenk, H. *Acta Crystallogr.* **1973**, *B29*, 1973.
(24) Erickson, L. E.; Ferrett, T. A.; Buhse, L. F. *Inorg. Chem.* **1983**, *22*, 1461.
(25) Sundquist, W. I.; Ahmed, K. J.; Hollis, L. S.; Lippard, S. J. *Inorg. Chem.* **1987**, *26*, 1524.
(26) Melanson, R.; Rochon, F. D. *Acta Crystallogr.* **1978**, *B34*, 941.
(27) Farrell, N. Private communication.
(28) Elding, L. I.; Groning, O. *Inorg. Chem.* **1978**, *17*, 1872.
(29) Jarvis, J. A. J.; Kilbourn, B. T.; Owston, P. G. *Acta Crystallogr.* **1971**, *B27*, 366.
(30) Melanson, R.; Hubert, J.; Rochon, F. D. *Acta Crystallogr.* **1976**, *B32*, 1914.
(31) Bodner, G. S.; Fernandez, J. M.; Arif, A. M.; Gladysz, J. A. *J. Am. Chem. Soc.* **1988**, *110*, 4082.
(32) Aris, K. R.; Brown, J. M.; Taylor, K. A. *J. Chem. Soc., Dalton Trans.* **1974**, 2222.
(33) Halpern, J. Reference 1, Chapter 5.
(34) Tomioka, K.; Nakajima, M.; Koga, K. *J. Am. Chem. Soc.* **1987**, *109*, 6213. Jacobsen, E. N.; Marko, I.; Mungall, W. S.; Schroeder, G.; Sharpless, K. B. *J. Am. Chem. Soc.* **1988**, *110*, 1968.

determined as much as kinetic as by equilibrium considerations. This is particularly critical for any proposed catalytic cycle. Clearly, several questions must be answered before the pronounced stereoselectivity reported here for the cis(N,olefin) isomers of mixed olefin-amino acid complexes containing chiral nitrogens can be employed to direct reliably the stereochemistry of reactions of coordinated prochiral olefins in the same molecule.

The relative ease with which 2-mb and allOH can be displaced by other olefins makes it readily possible to convert *cis*-Pt(sar)(2-mb)Cl and *cis*-Pt(*S*-pro)(2-mb)Cl to other cis(N,olefin) compounds in order to compare the degree of stereoselectivity for a series of prochiral olefins. The relative importance of the OH group, the length of the hydrocarbon chain, the degree of branching of the chain, and the effect of aromatic substituents can be determined by comparing the isomer ratios for such a series. Such efforts are currently being pursued in our laboratory to further clarify the role of specific structural features that are responsible for the extraordinary stereoselectivity which these compounds exhibit.

Acknowledgment is made to the donors of the Petroleum Research Fund, administered by the American Chemical Society, for support of this research, to the Pew Charitable Trust and the National Science Foundation for support for the NMR spectrometer used in this work, and to the Pew Mid-States Consortium for a Faculty Development Award (L.E.E.). The able assistance of Marufar Rahim (VT) and Peter Hayes (Grinnell) is gratefully acknowledged.

Supplementary Material Available: For the three structures reported, additional illustrations of NMR spectra (^1H, ^{13}C, ^{195}Pt) of some of the amino acid-olefin complexes and tables listing crystal data, anisotropic thermal parameters of the non-hydrogen atoms, and atomic coordinates and isotropic thermal parameters of the hydrogen atoms (7 pages); tables of observed and calculated structure factors (29 pages). Ordering information is given on any current masthead page.

Contribution from the URA 405 du CNRS, Electrochimie et Physico-Chimie des Complexes et des Systèmes Interfaciaux, and IBMC du CNRS, Laboratoire de Cristallographie Biologique, Institut de Chimie, Université Louis Pasteur, 1, rue Blaise Pascal, B.P. 296R8, 67008 Strasbourg Cedex, France

Trinuclear Copper(II) Hydroxo and Hexanuclear Copper(II) Oxo Complexes with the Ligand 3-(Benzylimino)butanone 2-Oxime. Syntheses and Spectral, Structural, and Redox Characteristics

Y. Agnus,* R. Louis, B. Metz, C. Boudon, J. P. Gisselbrecht, and M. Gross

Received December 28, 1990

The syntheses, structures, and properties of a trinuclear copper(II) hydroxo complex and a hexanuclear copper(II) oxo complex containing the same imino-oximato ligand are reported. The pair $[Cu_3(\mu_3\text{-}OH)L_3(ClO_4)_2(H_2O)]$ (**1**) and $[Cu_6(\mu_4\text{-}O)_2L_6(H_2O)](ClO_4)_2\cdot 0.5H_2O$ (**2**) displays the first example of tri- and hexacopper(II) complexes built with the same ligand, 3-(benzylimino)butanone 2-oxime (LH). The X-ray crystallographic structures have been determined. **1** crystallizes in the monoclinic space group $P2_1/c$ (a = 15.350 (1) Å, b = 12.508 (1) Å, c = 21.439 (2) Å, β = 96.81 (1)°, Z = 4). The molecular structure shows that the copper ions are at the corners of an equilateral triangle, separated by 3.25 Å, held together by a μ_3-hydroxo group and three oxime bridges. An unusual triply coordinated perchlorate ion interacts in axial position with the three copper ions. **2** crystallizes in the monoclinic space group $P2_1/n$ (a = 15.622 (2) Å, b = 27.025 (2) Å, c = 18.864 (4) Å, β = 97.38 (2)°, Z = 4). Here the $[Cu_6(\mu_4\text{-}O)_2L_6]^{2+}$ cation contains two triangular $[Cu_3O]$ units, bridged by their central oxygen atoms. The electron-transfer properties of **1** and **2** in propylene carbonate solution have been studied by voltammetry, coulometry, and spectrophotometry. **1** is electroreducible into a $[Cu^ICu^{II}_2(OH)]^+$ species at -0.41 V versus SCE, followed by a fast chemical step leading to another $[Cu^ICu^{II}_2(OH)]^+$ entity, **3**, which is reversibly oxidizable at +0.42 V versus SCE. **2** is reversibly electrooxidizable at +0.42 V versus SCE into a $[Cu^{III}Cu^{II}_2(O)]^{2+}$ species, **4**, which transforms slowly through an homogeneous reaction into **1**. Reversible and quantitative interconversion between **1** and **2** is achieved by protonation/deprotonation of the μ_3-oxygen. This proton gated reaction grants to the species either a mild oxidant (**1**) or a mild reductant (**2**) character. The similarity of the redox potential for the couples $[Cu^ICu^{II}_2(OH)]^+/[Cu^{II}Cu^{II}_2(OH)]^{2+}$ involving **3** and $[Cu^{II}_3(O)]^+/[Cu^{III}Cu^{II}_2(O)]^{2+}$ involving **2** makes **1** act as a chemical switch between two loops of redox reaction chains.

Introduction

Triangular copper(II) complexes have been extensively studied, especially regarding their magnetic, structural, and redox characteristics,[1-22] in relation to their interest in copper-proteins interactions and to homogeneous catalysis. μ-Hydroxo[1-20] or μ-oxo ions[6,15-22] have generally been observed as central bridging ligands. In the oxo derivatives, the oxygen atom is nearer the plane of the three copper ions (0.35 Å)[6] than in the hydroxo derivatives (0.48-0.93 Å).[4-6,8-10,12,13,16] These complexes exhibit identical, all different, or only two different copper stereochemistries. The coordination polyhedron of each metallic ion is a distorted octahedron. The three equatorial arrays are usually nearly coplanar, although orthogonal orientation with respect to the [3Cu] plane have been reported.[7-12]

Electrochemical studies have shown that monoelectronic transfers are possible: the $[Cu_3(\mu\text{-oxo})]$ groups are electrooxidizable,[18-21] generating $[Cu^{III}Cu^{II}_2]$ complexes, whereas the $[Cu_3(\mu\text{-hydroxo})]$ groups are electroreducible to $[Cu^ICu^{II}_2]$ compounds.[19,20]

* To whom correspondence should be addressed at Institut de Chimie, Université Louis Pasteur.

(1) Green, R. W.; Svasti, M. C. K. *Aust. J. Chem.* **1963**, *16*, 356-359.
(2) Beckett, R.; Colton, R.; Hoskins, B. F.; Martin, R. L.; Vince, D. G. *Aust. J. Chem.* **1969**, *22*, 2527-2533.
(3) Hoskins, B. F.; Vince, D. G. *Aust. J. Chem.* **1972**, *25*, 2039-2044.
(4) Beckett, R.; Hoskins, B. F. *J. Chem. Soc., Dalton Trans.* **1972**, 291-295.
(5) Hulsbergen, F. B.; ten Hoedt, R. W. M.; Verschoor, G. C.; Reedijk, J.; Spek, A. L. *J. Chem. Soc., Dalton Trans.* **1983**, 539-545.
(6) Butcher, R. J.; O'Connor, C. J.; Sinn, E. *Inorg. Chem.* **1981**, *20*, 537-545.
(7) Comarmond, J.; Dietrich, B.; Lehn, J. M.; Louis, R. *J. Chem. Soc., Chem. Commun.* **1985**, 74-76.
(8) Costes, J. P.; Dahan, F.; Laurent, J. P. *Inorg. Chem.* **1986**, *25*, 413-416.
(9) Kwiatkowski, M.; Kwiatkowski, E.; Olechnowicz, A.; Ho, D. M.; Deutsch, E. *Inorg. Chim. Acta* **1988**, *150*, 65-73.
(10) Ahlgren, M.; Turpeinen, U.; Smolander, K. *Acta Crystallogr., Sect. B* **1980**, *B36*, 1091-1095.
(11) Butcher, R. J.; Overman, J. W.; Sinn, E. *J. Am. Chem. Soc.* **1980**, *102*, 3276-3278.
(12) Smolander, K. *Acta Chem. Scand.* **1983**, *A37*, 5-13.
(13) Bailey, N. A.; Fenton, D. E.; Moody, R.; Scrimshire, P. J.; Beloritzky, E.; Fries, P. H.; Latour, J. M. *J. Chem. Soc., Dalton Trans.* **1988**, 2817-2824.

0020-1669/91/1330-3155$02.50/0